Modelling spatio-temporal soil moisture dynamics in mountain tundra

Tyystjärvi, Vilna

2021

Tyystjärvi , V , Kemppinen , J , Luoto , M , Aalto , T , Markkanen , T , Launiainen , S , Kieloaho , A-J & Aalto , J 2021 , ' Modelling spatio-temporal soil moisture dynamics in mountain tundra ' , Hydrological Processes , vol. 36 , no. 1 , pp. e14450 . https://doi.org/10.1002/hyp.14450

http://hdl.handle.net/10138/351584
https://doi.org/10.1002/hyp.14450

unspecified
acceptedVersion

Modelling spatio-temporal soil moisture dynamics in mountain tundra

Vilna Tyystjärvi[1,2] | Julia Kemppinen[3] | Miska Luoto[1] | Tuula Aalto[2] | Tiina Markkanen[2] | Samuli Launiainen[4] | Antti-Jussi Kieloaho[4] | Juha Aalto[1,2]

[1]Department of Geosciences and Geography, University of Helsinki, P.O. Box 64, 00014 University of Helsinki, Finland

[2]Finnish Meteorological Institute, P.O. Box 503, 00101 Helsinki, Finland

[3]Geography Research Unit, University of Oulu, P.O. Box 3000, 90014 Oulu, Finland

[4]Nature Resources Institute Finland, Latokartanonkaari 9, 00790 Helsinki, Finland

Correspondence
Vilna Tyystjärvi, Department of Geosciences and Geography, University of Helsinki, P.O. Box 64, 00014 University of Helsinki, Finland
Email: vilna.tyystjarvi@helsinki.fi

Funding information

Soil moisture has a fundamental influence on the processes and functions of tundra ecosystems. Yet, the local dynamics of soil moisture are often ignored, due to the lack of fine resolution, spatially extensive data. In this study, we modelled soil moisture with two mechanistic models, SpaFHy (a catchment-scale hydrological model) and JSBACH (a global land surface model), and examined the results in comparison with extensive growing-season field measurements over a mountain tundra area in northwestern Finland. Our results show that soil moisture varies considerably in the study area and this variation creates a mosaic of moisture conditions, ranging from dry ridges (growing season average 12 VWC%, Volumetric Water Content) to water-logged mires (65 VWC%). The models, particularly SpaFHy, simulated temporal soil moisture dynamics reasonably well in parts of the landscape, but both underestimated the range of variation spatially and temporally. Soil properties and topography were important drivers of spatial variation in soil moisture dynamics. By testing the applicability of two mechanistic models to predict fine-scale spatial and temporal variability in soil moisture, this study paves the way towards understanding the functioning of tundra ecosystems under climate change.

KEYWORDS
soil moisture, Arctic, tundra, hydrological modelling

1 | INTRODUCTION

Soil moisture is a crucial part of the hydrological cycle, influencing interactions between the land surface and atmosphere (Robock et al., 2000; Koster et al., 2004; Seneviratne et al., 2010). In mountain tundra, the importance of soil moisture is highlighted in its connection with vegetation patterns and Earth surface processes (Aalto et al., 2013; le Roux et al., 2013). It is also strongly linked to plant performance and ecosystem functionality, emphasising its ecological relevance under contemporary climate change (Bjorkman et al., 2018). Tundra ecosystems are characterised by a short but intensive growing season and a prolonged snowmelt period, which is strongly correlated with local topography (Niittynen et al., 2018). In cold climates, topography also influences the distribution of a spatially uneven organic layer (Seibert et al., 2007; Zhu et al., 2019). Processes linked to climate, varying topography and vegetation characteristics interact with soil moisture, causing spatial and temporal variation in its fine-scale patterns (Kemppinen et al., 2018; Penna et al., 2009).

At large scales, the spatio-temporal variation of soil moisture follows general climatic conditions (Seneviratne et al., 2010). However, at finer scales, its patterns are controlled by various landscape characteristics as well as local climate. Water flows within and above ground are controlled partly by soil hydraulic properties, topography and intensity of precipitation, while evapotranspiration is influenced by vegetation characteristics and radiation (Western et al., 2002; Seneviratne et al., 2010). These fine-scale variations of soil moisture can be considerable, particularly in heterogeneous landscapes, such as in mountain tundra, and need to be understood when considering area-averaged soil moisture variations at larger scales (Western et al., 2002). They also have important local ecosystem impacts. Spatio-temporal variations of soil moisture are an important driver of greenhouse gas fluxes (Lohila et al., 2016; Virkkala, 2020) as well as fine-scale patterns of vegetation properties (le Roux et al., 2013; Kemppinen, 2020). Therefore, through various feedback mechanisms, soil moisture in the tundra plays an important role in global change and its accurate predictions are fundamental to our ability to understand tundra ecosystems now and in the future.

Mechanistic models are useful tools in examining dynamic and complex processes, such the hydrological cycle (Abbott et al., 1986; Fatichi et al., 2016). Models depicting soil moisture dynamics have been developed for various applications, such as estimating global wetland areas, improving catchment scale flood forecasts and simulating fine-scale species distribution patterns (Berthet et al., 2009; Maclean et al., 2012; Zhang et al., 2016). Therefore, the level of detail in how and which hydrological processes are described varies even amidst similar models such as land surface models (Dirmeyer et al., 2006; Koster et al., 2009; Romano, 2014). As a result, model comparison and evaluation studies have found considerable differences when simulating soil moisture and its dynamics (Dirmeyer et al., 2004; Koch et al., 2016; Yuan and Quiring, 2017). In mountain tundra, where landscape heterogeneity is an important aspect of soil hydrology, evaluating soil moisture model performances requires spatially detailed measurements. Recent developments of *in situ* measurement techniques have improved the spatio-temporal resolution in which soil moisture can be measured and in turn provide more a comprehensive understanding of soil moisture dynamics and model performances (Kopecký et al., 2021; Vereecken et al., 2014; Wild et al., 2019).

The objectives of this study are to 1) quantify the spatio-temporal variability of soil moisture and its drivers in mountain tundra and 2) evaluate soil moisture simulations of two mechanistic models using high-resolution soil moisture field measurements. To the best of our knowledge, this is the first time that extensive, high-resolution observation data are used in detailed model-based analysis to unravel the mountain tundra soil moisture variability and drivers. One of the models, JSBACH, has been developed for use with large-scale climate models and concentrates on interactions between the land surface and atmosphere (Reick et al., 2013). Understanding how variation in landscape characteristics realises itself in model results is important in order to better understand what uncertainties relate to large-scale simulations of the land surface. The other one, Spatial Forest Hydrology Model (SpaFHy), has been developed for simulating catchment-level hydrology in boreal forests (Launiainen et al., 2019). The soil moisture estimations in sloping terrain with patchy soil and vegetation require specific capabilities from models, some of which are found in the more soil-vegetation oriented models and some in hydrology oriented models. Here we assess the impact of soil type, layers and implementation of topographical redistribution on soil moisture variation and test the models' ability to characterise the spatial and temporal variation of soil moisture with literature-based parameters. We also use a statistical model to examine which environmental variables, namely soil, topography and vegetation, contribute most to the soil moisture variation, and whether these controls are well addressed in the models.

2 | MATERIALS AND METHODS

2.1 | Study area

The study area is located in a valley between Mount Saana and Mount Jehkas in northwestern Fennoscandia (69°03' N 20°51' E, Fig. 1). The region experiences a subarctic climate with monthly average temperatures ranging from -12.9 °C in January to 11.2 °C in July (averages during 1981–2010; Pirinen et al., 2012). The total annual precipitation is 487 mm and snow covers the ground largely from October to May, although late-lying snowpacks can persist far into the summer. The landscape is characterised by varying vegetation (Riihimäki et al., 2019), soil type, geomorphology (le Roux and Luoto, 2014) and topography (Kemppinen et al., 2018). Vegetation consists mainly of dwarf-shrub dominated mountain heath with sporadic meadows and mires (Kemppinen et al., 2018; Riihimäki et al., 2019). The ground surface consists of thin mineral and organic soil layers that are partly covered by eroded boulders and exposed bedrock. Tundra mires with thicker layers of organic soil have formed mainly in the valley and flat upland areas in the west. The environmental variation is driven by fine-scale variation of topography, with relative elevation difference reaching nearly 250 meters (Aalto et al., 2013; le Roux et al., 2013).

[Insert Figure 1]

2.2 | Study setting

In this study, we measured the local variation of top soil moisture using 50 soil moisture loggers (TMS-4 datalogger; TOMST s.r.o., Prague, Czech Republic). They were installed in June 2018 and their locations recorded with an accuracy ≤ 6 cm using a hand-held Global Navigation Satellite System (GeoExplorer GeoXH 6000 Series; Trimble Inc., Sunnyvale, CA, USA). The loggers were situated to represent the entire soil moisture gradient of the landscape (Fig. 1) based on previous field studies in the area, with particular attention paid to the extremes: the water-logged peatlands (average soil moisture level > 60 VWC% (Volumetric Water Content); 10 loggers) and the dry ridges and mountain tops (< 15 VWC%; 10 loggers) (Happonen et al., 2019; Kemppinen et al., 2018, 2021). Some of the loggers are situated close to each other rather than evenly around the study area in order to describe the very fine-scale patterns of soil moisture variation caused by the spatially heterogeneous soil properties and topography of mountain tundra. They measure moisture to a depth of c. 14 cm below ground at 15 minute intervals (Wild et al., 2019). In the data processing, the raw time-domain transmission data were calibrated into VWC using a conversion tool provided by the manufacturer. The measurement uncertainties related to these loggers and their calibration have been discussed in Wild et al. (2019).

Calibration curves were chosen based on field-quantified soil moisture measurements recorded with a hand-held time-domain reflectometry sensor (FieldScout TDR 300; Spectrum Technologies Inc., Plainfield, IL, USA) during summer 2018 (four measurement campaigns in July–August). Of the 50 loggers, two were excluded from the analyses since they had dislocated during the study period. Thus the final data consisted of 48 loggers.

2.3 | Model input data

[Insert Table 1]

Environmental data required by SpaFHy and JSBACH were obtained from remote sensing techniques and field surveys (Table 1). The soil data, consisting of a rasterized classification of the surficial deposits (Fig. 1) and point measurements of the mineral and organic layer depths, have been described in detail by Kemppinen et al. (2018). In the brief, the surficial deposit map was created using field surveys and aerial images (0.5 m * 0.5 m resolution) provided by the National Land Survey of Finland. Three layer depth measurements in a 1 m * 1 m plot were taken every 50 meters from the whole study area. Three soil types were then defined for both models. Glacial till, fluvial deposits and boulders from the surficial deposits map were classified as mineral soils and peat deposits as peat soils. A third soil type was defined as a mixture of organic and mineral soil based on the average proportion of each layer. This soil type was classified as a combination from the surficial deposits map and vegetation type map as meadow and mire vegetation overlaying mineral soil (glacial till, fluvial deposits or boulders). Soil parameters for SpaFHy were kept close to those used in Launiainen et al. (2019). While a full sensitivity analysis for soil parameters was outside the scope of this study, we adjusted the field capacity in peat soils following a sensitivity analysis (Figure A1). This was done because the original parameters led to noticeably drier VWC% which is likely due to differences in peat soil properties in this study area. Soil type specific parameters for JSBACH were taken from Hagemann and Stacke (2015) (Table A1).

Both models describe vegetation by type and coverage. To create a raster of vegetation types, we utilised a Random Forest (RF) model trained by vegetation observations and five PlanetScope images (resolution 3 m * 3 m) from growing season 2018 (Breiman, 2001; Planet Team, 2017). The RF model was run 100 times by bootstrapping the training data. The final pixel values were determined as the most common class value from a five-class vegetation classification including meadows, deciduous shrubland, evergreen shrubland, barren tundra and wetlands. In SpaFHy, the parameters (Table A1) for these classes were obtained from the literature (Launiainen et al., 2019; Lin et al., 2015; Pop et al., 2000; Starr et al., 2008). In JSBACH, we used the plant functional types of peatland (wetland class), C3 grass (meadow class) and tundra (deciduous and evergreen shrubland) with their default parameter values (Kattge et al., 2009; Knorr et al., 2010). To estimate vegetation cover, we calculated the Normalized Difference Vegetation Index (NDVI) from a Sentinel-2 image taken in August 2019 (ESA, 2021) using Eq. (1)

$$NDVI = \frac{NIR - red}{NIR + red} \tag{1}$$

where NIR and red refer to the near infrared and red bands (Huete et al., 2002). For SpaFHy, the maximum leaf area index (LAI) was then calculated from NDVI and the vegetation type map based on an approach by Street et al. (2007).

Topography variables were calculated from a LiDAR-based (light detection and ranging) Digital Elevation Model (DEM; horizontal resolution 2 m *2 m, vertical resolution 30 cm; NLS, 2020). SAGA Wetness Index (SWI) (Böhner and Selige, 2006) can be used as a proxy for soil moisture similarly as the original Topographic Wetness Index (TWI) (Beven and Kirkby, 1979). However, SWI is an algorithm specific to SAGA GIS (Conrad et al., 2015) and is a modified version of the Multiple-flow Freeman algorithm (FD8f) (Freeman, 1991). Different from FD8f, SWI uses a modified catchment area. Thus, SWI produces a spatially smoothed TWI distribution, that is, a smooth stream network (Kopecký et al., 2021). This means that compared to the original TWI, SWI allows low-lying flat areas close to flow channels to have higher index values (Böhner and Selige, 2006). We calculated SWI using t-value 10 (that is, the suction effect) and a filled DEM following Wang and Liu (2006) in SAGA GIS hydrology module (Böhner and Antonić, 2009) with specific catchment area and local slope methods following Eq. (2)

$$SCA_M = SCA_{max} \frac{1}{20}^{\beta exp(20^{\beta})} for SCA < SCA_{max} \frac{1}{20}^{\beta exp(20^{\beta})}$$
$$SWI = ln \frac{SCA_M}{tan(\beta)} \tag{2}$$

where SCA and SCA_M are the specific and modified specific catchment areas, β is the slope angle and $tan(\beta)$ is the local slope (Böhner and Selige, 2006).

The shadowing influence of topography on incoming solar radiation was calculated for each month of the year from the DEM using the potential incoming solar radiation module with a sky view factor option and lumped atmospheric transmittance in the RSAGA package (Böhner and Antonić, 2009). The monthly values were then divided by the potential radiation received by a flat surface in the same latitude, and interpolated to obtain daily correction factors for incoming solar radiation at each grid-cell for both models.

The meteorological data for January 2015–September 2019 were obtained from the Finnish Meteorological Institute's Kilpisjärvi kyläkeskus meteorological station (69°02' N 20°47' E, 480 m a.s.l.; Finnish Meteorological Insitute, 2020) ca. 1.5 km southwest from the centre of the study area. The daily variables used were air temperature (°C), precipitation (mm d^{-1}), relative humidity (%), wind speed (m s^{-1}), wind direction (°) and air pressure (hPa). Global radiation (W m^{-2}) was extracted from the 10 km * 10 km gridded dataset provided by Finnish Meteorological Insitute (2019).

2.4 | Models

2.4.1 | SpaFHy

The Spatial Forest Hydrology Model (SpaFHy) is a semi-distributed hydrological model developed to simulate evapotranspiration and water balance in a boreal forest landscape (Launiainen et al., 2019). It has been tested both at the plot and at the catchment level at various sites in Finland, including a catchment similar to this study area. SpaFHy consists of three submodules that simulate water balance above ground, within topsoil and within the catchment. Above-ground processes are included in the canopy module, which describes the processes related to vegetation, ground surface and snowpack. Vegetation is divided into classes, which in this study include deciduous and coniferous shrubland and mire vegetation. These differ mainly in their seasonal cycle, water usage and photosynthetic capacities. Soil moisture is depicted as a two-layer bucket model which consists of an organic top layer and a root layer. The organic top layer is a shallow layer (4 cm) with soil properties similar to peat soils. The root layer depth was set to 20 cm to keep it close to the measured soil moisture. Finally, the TOPMODEL submodule links the grid cell water balance conceptually with the catchment-scale water balance through the subsurface storage bucket. The saturation deficit of each grid cell is linked to the average saturation deficit of the whole catchment subsurface storage so that grid cells with higher index values, in this study SWI values, are more likely to be saturated (Launiainen et al., 2019). This allows accumulation of soil water in lowland areas with high SWI values and dynamic formation of water-saturated areas. Using SWI instead of TWI means that soil water should accumulate more evenly in flatland areas with high index values. In general, this modelling approach allows recognising and describing the landscape-level heterogeneity in biogeophysical conditions through geospatial data and remote sensing methods and linking this variability to a spatially explicit mechanistic model in order to better understand landscape-level hydrological processes.

SpaFHy was run in daily time steps as a catchment-scale version. For input data, it requires raster files of maximum LAI for each vegetation class, as well as canopy height, soil type, SWI and masks of the catchment area and water bodies. Spatial resolution was set to 10 m * 10 m. Canopy height was set to 0.5 m as its influence is negligible in low vegetation (Launiainen et al., 2019).

2.4.2 | JSBACH

JSBACH is the land surface model of the Max Planck Institute for Meteorology (MPI-M) Earth System Model (Giorgetta et al., 2013; Reick et al., 2013). It describes processes involved in the interactions between the lower level of the atmosphere and land surface and has been used in several studies simulating biogeophysical and -chemical processes, including hydrological research (Gößling and Reick, 2011; Gao et al., 2016; Heidkamp et al., 2018). Structurally, JSBACH consists of several submodules that describe the terrestrial energy balance, heat transfer and water budget, vegetation dynamics and phenology, carbon cycle over land, land cover change and surface albedo (Böttcher et al., 2016; Groner et al., 2018; Hagemann and Stacke, 2015; Heidkamp et al., 2018; Raddatz et al., 2007; Thum et al., 2011). Vegetation is described through plant functional types, which are included in each grid cell as overlapping tiles. Each grid cell, of user-defined resolution, can thus have several vegetation types.

In JSBACH, the vertical movement of soil moisture is depicted through one-dimensional Richard's equation which is typically used in soil moisture modelling to study processes related to interactions between land surface and atmosphere (Romano, 2014). In the new hydrology scheme developed by Hagemann and Stacke (2015), the soil profile consists of five layers with increasing depths up to 10 m, improving descriptions of bare soil evaporation and soil moisture buffering. Soil properties in each layer are kept constant. The actual soil depth is controlled through a soil depth variable and a root depth variable controls the depth from which transpiration may occur. Water flow between grid cells is not accounted for and each grid cell acts as a separate hydrological unit.

Here, JSBACH was run as an offline version with user-generated meteorological forcing data with modules bethy, phenology, albedo and yasso turned on. The model was run over 210 independent grid cells to allow for spatial variation in the input data, namely in soil properties, vegetation characteristics and topographical shading of solar radiation. Unlike in global simulations with spatially averaged soil properties, specific soil classes were used to describe conditions in the landscape. Surface parameters were taken from Hagemann (2002) using parameters for fens and bogs, upland tundra and polar deserts (Table A1). Minimum soil and rooting depths were set to 0.5 m as soil depths less than 0.5 m led to negligible transpiration and canopy conductance rates. A spin-up run of three years prior to the study period was performed for both models in order to equilibriate slowly changing variables. To visualize spatial variation in JSBACH, the point-based results were mapped to matching environmental conditions in the study area.

2.4.3 | Statistical model

Field data was used to address the drivers of soil moisture variation using a Generalised Additive Model (GAM). It allows for non-linearity in the relationship between response and predictor variables by splitting the regression line into segments to which the regression line is fitted using a user-controlled smoothing function (Hastie and Tibshirani, 1987). We modelled the spatial variation of growing season average soil moisture and the temporal range of variation (growing season maximum VWC% - growing season minimum VWC%) as a function of organic soil depth (up to 80 cm), vegetation cover (%), topographical shading of incoming solar radiation, elevation and SWI. The variables describing soil and topography are commonly used in soil moisture research (Kemppinen et al., 2018; Williams et al., 2009). Vegetation cover has a more complex relationship with soil moisture but was used as a predictor variable due to its influence on temporal soil moisture dynamics in the mechanistic models used in this study.

The model was fitted using the mgcv package in R (version 3.4.4; Wood, 2011; R Development Core Team, 2020), with maximum degrees of smoothing restricted to three. The response variables were log-transformed to approximate normal distribution and then transformed back before plotting them. Effect sizes for each predictor were calculated based on the predicted minimum and maximum VWC% and range of VWC% over the field data while other terms were held constant at their mean values. To quantify observation-related uncertainty in model estimates, we used a bootstrap sampling with 200 repetitions. A similar model was developed for the results of SpaFHy and JSBACH using soil porosity, vegetation cover, SWI (in SpaFHy) and solar radiation as the predictor variables in order to estimate the influence of these variables in the mechanistic models.

2.5 | Analysis of results

The measurements and model simulations were grouped into three regimes in order to reduce uncertainty related to the accuracy of single logger data and to examine temporal variation of soil moisture. As soil conditions influenced the logger and model average VWC% considerably (Fig. A2), the field measurements were classified based on organic layer depth to xeric (organic depth < 5 cm, 20 loggers), mesic (organic depth 5–25 cm, 18 loggers) and hydric (organic depth > 25 cm, 10 loggers) regimes. Model results were classified similarly based on soil type. Growing-season months with no extensive snow cover (July–September) in 2018 and 2019 were selected for further analysis. For JSBACH, the weighted average VWC% of the top two soil layers (6 and 25 cm thick) was calculated (center depth 16 cm), and the same was done for SpaFHy for the top and root zone layers (center depth 12 cm)(Table A1). In order to estimate soil moisture variation in the landscape, we calculated growing season averages from July–September 2018–2019 and used range of variation VWC% of the same time period as a measure of temporal variation. To show the temporal correlation between the timeseries of modelled and measured VWC%, measurements and model ouputs were averaged over the regimes. Then the growing season average of each timeseries was deducted from each averaged timeseries for simpler plots and the amount of explained variance (R^2) by a linear regression model was calculated in each regime.

3 | RESULTS

3.1 | Temporal variation of soil moisture

The temporal patterns of soil moisture are distinctively different among the moisture regimes (Fig. 2, Fig. A3 and Table 1). According to field measurements, the xeric regime has on average 14 VWC% throughout the growing season. There is little variation in the VWC% but clear short-term responses to precipitation events. In the mesic regime, average VWC% is 26 %, and in the hydric regime 61 %. Variation between growing season months is higher in the hydric regime, with August being the driest month (10 VWC% variation). In the xeric and mesic regimes, monthly averages are nearly constant (1–2 VWC% variation) and range of variation over the whole growing season is low (15 VWC%). Apart from one logger, the time series measured in the xeric regime are closer to each other compared to the hydric and mesic regimes.

[Insert Figure 2]

The modelled temporal variation of soil moisture followed the characteristics of these regimes reasonably closely

(Fig. 2 and Fig. 3). Average growing season soil moisture ranged between 17–60 VWC% in JSBACH and 15–48 VWC% in SpaFHy (Table 2). Modelled range of variation was lower than the measured range in all regimes, with JSBACH closer to measurements in the mesic (JSBACH 12 VWC%, measured 16 VWC%) and hydric (12 VWC% and 44 VWC%) regimes and SpaFHy in the xeric regime (10 VWC% and 15 VWC%). Variation between monthly averages was low (< 3 VWC%) in all regimes, although variation was higher in the hydric regime than in the xeric and mesic regimes. The minimum values in SpaFHy's hydric regime decreased notably compared to average values, otherwise the minimum and maximum values in both models were close to regime averages (Fig. 2).

[Insert Table 2]

The correlation between modelled and measured timeseries also depended on the moisture regime (Fig. 3). The highest R^2 for both models (0.60 for JSBACH and 0.72 for SpaFHy) was in the hydric regime while R^2 values in the xeric regime were around 0.5–0.6. However, in the mesic regime the results were more scattered, and thus, R^2 was lower for both models. The slopes for both models in the hydric regime were fairly large, indicating that while the models are capable of producing the temporal patterns, their magnitudes are smaller compared to measurements. SpaFHy's R^2 was higher than JSBACH in all regimes but it also had higher slopes in all regimes.

[Insert Figure 3]

3.2 | Spatial variation in soil moisture

[Insert Figure 4]

Spatial variation of soil moisture in the landscape was considerable (Fig. 4). Both model results and field measurements showed that dry conditions (15 – 20 VWC%) dominate the landscape while wetter regimes (> 20 VWC%) are concentrated mostly in flatter areas in the west and in the valley between the two fells. However, modelled spatial variability of soil moisture across the landscape was smaller than observed, with model results concentrating close to regime averages and measured averages spread more evenly between regime averages.

Temporal variation was generally higher (range > 25 VWC%) in wetter areas in the field measurements. However, range in field measurements was more scattered, with some drier (wetter) loggers also showing high (low) temporal variation (average VWC 15 % (75 %) and range 45 % (15 %)). In the model results however, there was significantly less temporal variation in general, with maximum range values below 20 VWC%. In both models, wetter areas had generally higher temporal variation as well.

The statistical model GAM explained 79 % of the spatial variation in average soil moisture (Fig. 5). Organic layer depth controlled a large part of the variation (effect size 29 VWC%) with thin organic layers resulting in lower VWC. In thick organic layers (> 50 cm) the fitted function was associated with large uncertainty, partly due to fewer measurements. The second most influential variable was SWI (effect size 22 VWC%), which also had a positive relationship with VWC, meaning that high SWI values, found in lowlands and local depressions, had on average higher VWC% than upland areas. Other variables had only a minor or no clear effect on average soil moisture. In SpaFHy and JSBACH, only soil porosity had any notable effect on the average VWC% (effect size 36 VWC% and 42 VWC% respectively).

GAM explained 44 % of the temporal variation in the data. Organic layer depth and SWI had the largest effect sizes (42 and 11 VWC% respectively). Other variables had no clear effects. In SpaFHy, vegetation cover had the strongest influence on range of variation (effect size 7 VWC%), while in JSBACH soil type played the most important role (effect size 8 VWC%).

[Insert Figure 5]

4 | DISCUSSION

Our study shows that soil moisture exhibits considerable spatial and some temporal variation in the study area, creating distinct moisture regimes (Fig. 2 and Fig. 4). Most of the study area is characterised by dry average moisture conditions (xeric regime) in which there is little variation between monthly averages during the growing season. Wetter moisture conditions, including mesic and hydric regimes, are found in low-lying and depression areas with thicker organic soil layers (> 25 cm) and exhibit higher average moisture conditions. There is greater temporal variation, particularly in the hydric regime. This is partly due to the lower water retention ability of coarse mineral soils compared to soils with more organic material.

The mechanistic models capture parts of the temporal variation fairly well (Fig. 2 and Fig. 3). Spatial and temporal variation is similar in all three moisture regimes. In the xeric regime, the responses to precipitation events are similar in the models and measurements, although JSBACH in particular underestimates the range of variation (Table 2). In the mesic and hydric regimes, the average time series show little temporal variation compared to measurements, although SpaFHy's minimum values follow a similar monthly pattern as the measurements (Fig. 2). While average temporal and spatial patterns are similar in the models and measurements, both models underestimated the range of variation. Particularly temporal variation might benefit from adjusting soil properties in the model simulations. However, we wanted to retain the existing features and scalability of the regional model. Further, removing the cause of the lack of variation in a proper way might require more than just parameter tuning, including re-think of the model set-up for vegetation and soil.

Previous studies in the study area have linked the fine-scale spatial variation of soil moisture to the environmental gradients of the landscape, such as the varying topographical conditions and soil properties (Kemppinen et al., 2018). Our results indicate that a large part of the spatial variation of soil moisture can be attributed to soil properties (Fig. 5). Thin mineral soils are not as efficient at retaining water as thick organic soils, and in turn, the former dry quickly after precipitation events compared to the latter, which stay more stable by retaining soil moisture (Legates et al., 2011; Migała et al., 2014). Although the importance of soil properties is also evident in the model results, it does demonstrate a common problem in hydrological process-models and soil properties. Soil properties can vary considerably over short distances, particularly in a landscape such as mountain tundra where the soil layer can be thin and the accumulation of soil organic matter depends on topography (Migała et al., 2014; Seibert et al., 2007). However, measuring this variability at a high spatial resolution and broad spatial extent is challenging, and consequently the input data in hydrological models cannot account for real variability in soil hydrological properties. This and the lack of spatial variation in the organic soil layer are likely to explain a large part of the underestimated spatio-temporal variation of modeled soil moisture (Fig. 4 and Fig. 5).

Vegetation seems to little to no effect on average VWC% or its temporal range (Fig. 5). Previous studies have shown that woody vegetation cover in particular can decrease soil moisture in the tundra (Kemppinen et al., 2021), for instance through increased transpiration (Pearson et al., 2013). The estimations on the influence of vegetation cover on the temporal variation of soil moisture seem to differ in SpaFHy and JSBACH, which might explain the lack of spatial variation in JSBACH (Fig. 4). Figure A4 shows that in JSBACH vegetation cover does influence transpiration. However, as transpiration extracts water first from a deeper soil depth, it does not instantaneously control soil moisture in the top soil layers. This leads to the apparently negligible influence of vegetation to the soil moisture in JSBACH.

Topography, here accounted through SWI, was found to influence spatial and temporal variability of soil moisture (Fig. 5). Mechanistically modelling this variation is possible on catchment level models such as SpaFHy, but in this study the influence of SWI on SpaFHy's results was small. This is likely because peatland areas in the study area are strongly concentrated in areas with high SWI, as organic matter accumulates in local depressions and flatlands, similarly to soil moisture (Fig. 1). However, high SWI values in particular could explain the lack of temporal variation in the hydric regime (Fig. 2), as the distribution of water in SpaFHy might cause these areas to be nearly constantly saturated. In JSBACH, the influence of hillslope level topography on soil hydrology is ignored as global land surface models focus on large-scale processes. However, hillslope level processes are important for land surface – atmosphere interactions and recent studies have focused on incorporating this subgrid variability in global scale models (Fan et al., 2019). Another aspect of topography that might be important in this study area is snow distribution. While typically most of the snow in the study area melts by May, the spatially and temporally uneven snowmelt period creates hydrologically distinct conditions such as meltwater streams and late-lying snowpacks, which in turn influence soil moisture far into the growing season (Niittynen et al., 2018; Sturm et al., 2005; Woo et al., 2006). Incorporating this variation into mechanistic models and examining its influence on soil moisture variation is an important future research question, as snow conditions are predicted to change considerably due to climate change (Bintanja and Andry, 2017; Fountain et al., 2012).

Previous research into soil moisture products has revealed that different outputs may not be intercomparable (Dirmeyer et al., 2006; Koster et al., 2009). In this study, we have compared three data sources for soil moisture and while the model parameters and input data have been harmonised in as much detail as the model structures allow, it is important to understand how these results differ from each other. Firstly, the field loggers describe soil moisture conditions in an exact point and are thus considerably influenced by for example fine-scale soil heterogeneity. In comparison, the input data resolution and model configuration in both SpaFHy and JSBACH mean that they describe moisture conditions in a larger area. Thus, comparing specific measurements to their matching model grids is not particularly helpful. Here, we have instead examined more generalised results by grouping both models and measurements to moisture regimes to diminish the uncertainty related to specific point measurements. Secondly, the soil moisture loggers describe topsoil conditions which interactions between land surface and atmosphere influence the most. In some areas of the study site, the soils are shallow enough, and thus, we can assume that the loggers describe the whole vertical soil moisture content which might not be the case in areas where soils are thick. The models also describe moisture deeper than what the loggers can reach (> 15 cm depth) and in a larger vertical space than the measurements. In SpaFHy, the root zone depth was set to 0.2 in order to make it more comparable with measurements and the average soil conditions in the study area. In areas with shallow soils, the results represent the measured conditions fairly well. However, for example in areas with deep peat deposits, the model does not take the influence of soil depth into account. In JSBACH, which does simulate the vertical moisture profile more explicitly, the model results have been calculated from the top two layers in order to make them more comparable with the measurements. However, the minimum depth of 0.5 m in JSBACH means that soil moisture variation in mineral soils particularly is dampened by buffering from deeper layers. These aspects may explain the relatively large slopes between modelled and measured timeseries (Fig. 3). To conclude, the models and measurements are not entirely comparable with each other from all perspectives. However, while the precise estimates of VWC may vary, the similarities and disparities between spatio-temporal dynamics of each product may still be compared and used to inform soil moisture dynamics (Koster et al., 2009; Saleem and Salvucci, 2002).

Our results show that in order to model the spatio-temporal variation of soil moisture accurately in mountain tundra, soil properties, including the thickness of the organic layer, are important. In spatially distributed models, such as SpaFHy, this requires developing methods to depict the soil organic layer and ways to infer soil hydrological properties at high spatial resolution. Recent advances in modelling spatial variation in soil properties based on DEMs (Li et al., 2020) could provide an option which should be further tested in mountain tundra. Another possibility is utilising remotely sensed soil moisture datasets to better understand its spatial variation (Mohanty et al., 2017; Manninen et al., 2021). Although global land surface models, such as JSBACH, cannot capture the fine-scale variation of soil properties or other environmental variables in a similar fashion to catchment-scale models, methods of describing sub-grid heterogeneity in such models do exist. In JSBACH, vegetation cover is described through tiles to allow for multiple plant functional types within one grid cell (Reick et al., 2013). Hydrologic response units have been used similarly to include variation in soil properties (Chaney et al., 2016). Description of the soil organic layer has also been found to be important in land surface models (Rinke et al., 2008; Ekici et al., 2015).

Considering temporal soil moisture dynamics, range of variability as a static measure ignores many aspects such as temporal resolution (whether the variation is linked solely to short-term variation in, for example, precipitation, or more seasonal variation) as well as temporal development in the land surface variables that influence soil moisture (such as vegetation phenology and snowmelt dynamics). These aspects can be included in mechanistic models as well as estimates of future changes in, for example, climate or vegetation patterns. Thus, our findings suggest that more effort should be made in considering local processes that influence soil moisture dynamics, possibly through a fusion of remote sensing, in situ data and mechanistic models. In a time of rapid environmental changes in the tundra, such methods will be fundamental in making dynamical future predictions on the functioning of Arctic ecosystems.

5 | CONCLUSIONS

To contribute to the understanding soil moisture dynamics in mountain tundra, we modelled its spatial and temporal variation using extensive field measurements and two mechanistic models, SpaFHy and JSBACH. We found substantial fine-scale spatial variation in soil moisture ranging from dry mineral soils to wet peatlands. By investigating the soil moisture dynamics, we identified distinct hydrological regimes over the landscape. Our results show that mechanistic models are able to simulate average VWC% conditions within the regimes but underestimate both temporal and spatial variation compared to measurements. Spatial variation of soil moisture was largely related to soil properties in both model simulations and measurements. Our results indicate that improving these descriptions as well as simulations of soil moisture variability in mechanistic models is needed to improve modelling of soil moisture dynamics in tundra ecosystems. The results are important for understanding uncertainties related to global and regional analyses and inform future model developments needed to understand the ecosystem consequences of the Arctic change.

Acknowledgements

The authors would like to thank Pekka Niittynen for his contribution to the preparation of the vegetation data. VT and JA were funded by the University of Helsinki through the MicroClim project (grant no. 7510145). We are grateful to the Academy of Finland (project 286950) for funding the field measurements, and for the BioGeoClimate Modelling lab and its field assistants, as well as the Carbon Cycle research group, for their help and support. JK was funded by the Arctic Interactions at the University of Oulu and Academy of Finland (grant no. 318930, Profi 4), Maa- ja metsätekniikan tuki ry., Tiina and Antti Herlin Foundation and Nordenskiöld-samfundet. TA was funded by Academy of Finland (grants no. 307331 and 641816), and Academy of Finland Flagship (grant no. 337552). TA and TM were funded by The Strategic Research Council at the Academy of Finland (312932), Academy of Finland (341752) and Ministry of Agriculture and Forestry (4400T-2105). SL and AK were funded by the Academy of Finland (no. 296116 & 327180).

references

Aalto, J., le Roux, P. C. and Luoto, M. (2013) Vegetation mediates soil temperature and moisture in arctic-alpine environments. *Arctic, Antarctic, and Alpine Research*, **45**, 429–439.

Abbott, M. B., Bathurst, J. C., Cunge, J. A., O'Connell, P. E. and Rasmussen, J. (1986) An introduction to the european hydrological system - systeme hydrologique europeen, "she", 1: History and philosophy of a physically-based, distributed modelling system. *Journal of hydrology*, **87**, 45–59.

Berthet, L., Andréassian, V., Perrin, C. and Javelle, P. (2009) How crucial is it to account for the antecedent moisture conditions in flood forecasting? comparison of event-based and continuous approaches on 178 catchments. *Hydrology and Earth System Sciences*, **13**, 819–831.

Beven, K. J. and Kirkby, M. J. (1979) A physically based, variable contributing area model of basin hydrology/un modèle à base physique de zone d'appel variable de l'hydrologie du bassin versant. *Hydrological Sciences Journal*, **24**, 43–69.

Bintanja, R. and Andry, O. (2017) Towards a rain-dominated arctic. *Nature Climate Change*, **7**, 263–267.

Bjorkman, A. D., Myers-Smith, I. H., Elmendorf, S. C., Normand, S., Rüger, N., Beck, P. S., Blach-Overgaard, A., Blok, D., Cornelissen, J. H. C., Forbes, B. C. et al. (2018) Plant functional trait change across a warming tundra biome. *Nature*, **562**, 57–62.

Böhner, J. and Antonić, O. (2009) Land-surface parameters specific to topo-climatology. *Developments in soil science*, **33**, 195–226.

Böhner, J. and Selige, T. (2006) Spatial prediction of soil attributes using terrain analysis and climate regionalisation. In *SAGA – Analysis and Modelling Applications* (eds. J. Böhner, K. McCloy and J. Strobl), vol. 115. Göttingen: Göttinger Geographische Abhandlungen.

Böttcher, K., Markkanen, T., Thum, T., Aalto, T., Aurela, M., Reick, C. H., Kolari, P., Arslan, A. N. and Pulliainen, J. (2016) Evaluating biosphere model estimates of the start of the vegetation active season in boreal forests by satellite observations. *Remote Sensing*, **8**, 580.

Breiman, L. (2001) Random forests. *Machine learning*, **45**, 5–32.

Chaney, N. W., Metcalfe, P. and Wood, E. F. (2016) Hydroblocks: a field-scale resolving land surface model for application over continental extents. *Hydrological Processes*, **30**, 3543–3559.

Conrad, O., Bechtel, B., Bock, M., Dietrich, H., Fischer, E., Gerlitz, L., Wehberg, J., Wichmann, V. and Böhner, J. (2015) System for automated geoscientific analyses (saga) v. 2.1.4. *Geoscientific Model Development*, **8**, 1991–2007.

Dirmeyer, P. A., Gao, X., Zhao, M., Guo, Z., Oki, T. and Hanasaki, N. (2006) Gswp-2: Multimodel analysis and implications for our perception of the land surface. *Bulletin of the American Meteorological Society*, **87**, 1381 – 1398.

Dirmeyer, P. A., Guo, Z. and Gao, X. (2004) Comparison, validation, and transferability of eight multiyear global soil wetness products. *Journal of Hydrometeorology*, **5**, 1011 – 1033.

Ekici, A., Chadburn, S., Chaudhary, N., Hajdu, L., Marmy, A., Peng, S., Boike, J., Burke, E., Friend, A., Hauck, C. et al. (2015) Site-level model intercomparison of high latitude and high altitude soil thermal dynamics in tundra and barren landscapes. *The Cryosphere*, **9**, 1343–1361.

ESA (2021) European space agency — products — sentinel-2. `https://sentinel.esa.int/web/sentinel/missions/sentinel-2/data-products`. Last access: 10 October 2020.

Fan, Y., Clark, M., Lawrence, D. M., Swenson, S., Band, L., Brantley, S. L., Brooks, P. D., Dietrich, W. E., Flores, A., Grant, G. et al. (2019) Hillslope hydrology in global change research and earth system modeling. *Water Resources Research*, **55**, 1737–1772.

Fatichi, S., Vivoni, E. R., Ogden, F. L., Ivanov, V. Y., Mirus, B., Gochis, D., Downer, C. W., Camporese, M., Davison, J. H., Ebel, B. et al. (2016) An overview of current applications, challenges, and future trends in distributed process-based models in hydrology. *Journal of Hydrology*, **537**, 45–60.

Finnish Meteorological Insitute (2019) Daily global radiation, 10km, 1961-2019, netcdf. URL: `https://etsin.fairdata.fi/dataset/95b5caa9-967f-4ede-a064-30d4b0a64f09`. Last access: 27 September 2020.

— (2020) Weather and sea - download observations. URL: `https://en.ilmatieteenlaitos.fi/download-observations`. Last access: 27 September 2020.

Fountain, A. G., Campbell, J. L., Schuur, E. A., Stammerjohn, S. E., Williams, M. W. and Ducklow, H. W. (2012) The disappearing cryosphere: impacts and ecosystem responses to rapid cryosphere loss. *BioScience*, **62**, 405–415.

Freeman, T. G. (1991) Calculating catchment area with divergent flow based on a regular grid. *Computers & Geosciences*, **17**, 413–422.

Gao, Y., Markkanen, T., Thum, T., Aurela, M., Lohila, A., Mammarella, I., Kämäräinen, M., Hagemann, S., Aalto, T. et al. (2016) Assessing various drought indicators in representing summer drought in boreal forests in finland. *Hydrology and Earth System Sciences*.

Giorgetta, M. A., Jungclaus, J., Reick, C. H., Legutke, S., Bader, J., Böttinger, M., Brovkin, V., Crueger, T., Esch, M., Fieg, K. et al. (2013) Climate and carbon cycle changes from 1850 to 2100 in mpi-esm simulations for the coupled model intercomparison project phase 5. *Journal of Advances in Modeling Earth Systems*, **5**, 572–597.

Gößling, H. and Reick, C. H. (2011) What do moisture recycling estimates tell? lessons from an extreme global land-cover change model experiment. *Hydrology and Earth System Sciences*, **8**, 3217–3235.

Groner, V., Raddatz, T., Reick, C. H. and Claussen, M. (2018) Plant functional diversity affects climate-vegetation interaction. *Biogeosciences*, **15**, 1947–1968.

Hagemann, S. (2002) *An improved land surface parameter dataset for global and regional climate models*. No. Report 336. Hamburg: Max-Planck-Institut für Meteorologie.

Hagemann, S. and Stacke, T. (2015) Impact of the soil hydrology scheme on simulated soil moisture memory. *Climate Dynamics*, **44**, 1731–1750.

Happonen, K., Aalto, J., Kemppinen, J., Niittynen, P., Virkkala, A.-M. and Luoto, M. (2019) Snow is an important control of plant community functional composition in oroarctic tundra. *Oecologia*, **191**, 601–608.

Hastie, T. and Tibshirani, R. (1987) Generalized additive models: some applications. *Journal of the American Statistical Association*, **82**, 371–386.

Heidkamp, M., Chlond, A. and Ament, F. (2018) Closing the energy balance using a canopy heat capacity and storage concept– a physically based approach for the land component jsbachv3. 11. *Geoscientific Model Development*, **11**, 3465–3479.

Huete, A., Didan, K., Miura, T., Rodriguez, E. P., Gao, X. and Ferreira, L. G. (2002) Overview of the radiometric and biophysical performance of the modis vegetation indices. *Remote sensing of environment*, **83**, 195–213.

Kattge, J., Knorr, W., Raddatz, T. and Wirth, C. (2009) Quantifying photosynthetic capacity and its relationship to leaf nitrogen content for global-scale terrestrial biosphere models. *Global Change Biology*, **15**, 976–991.

Kemppinen, J. (2020) *Soil moisture and its importance for tundra plants*. Ph.D. thesis, University of Helsinki, Helsinki.

Kemppinen, J., Niittynen, P., Riihimäki, H. and Luoto, M. (2018) Modelling soil moisture in a high-latitude landscape using lidar and soil data. *Earth Surface Processes and Landforms*.

Kemppinen, J., Niittynen, P., Virkkala, A.-M., Happonen, K., Riihimäki, H., Aalto, J. and Luoto, M. (2021) Dwarf shrubs impact tundra soils: Drier, colder, and less organic carbon. *Ecosystems*, 1–15.

Knorr, W., Kaminski, T., Scholze, M., Gobron, N., Pinty, B., Giering, R. and Mathieu, P.-P. (2010) Carbon cycle data assimilation with a generic phenology model. *Journal of Geophysical Research: Biogeosciences*, **115**.

Koch, J., Cornelissen, T., Fang, Z., Bogena, H., Diekkrüger, B., Kollet, S. and Stisen, S. (2016) Inter-comparison of three distributed hydrological models with respect to seasonal variability of soil moisture patterns at a small forested catchment. *Journal of Hydrology*, **533**, 234–249.

Kopecký, M., Macek, M. and Wild, J. (2021) Topographic wetness index calculation guidelines based on measured soil moisture and plant species composition. *Science of The Total Environment*, **757**, 143785.

Koster, R. D., Dirmeyer, P. A., Guo, Z., Bonan, G., Chan, E., Cox, P., Gordon, C., Kanae, S., Kowalczyk, E., Lawrence, D. et al. (2004) Regions of strong coupling between soil moisture and precipitation. *Science*, **305**, 1138–1140.

Koster, R. D., Guo, Z., Yang, R., Dirmeyer, P. A., Mitchell, K. and Puma, M. J. (2009) On the nature of soil moisture in land surface models. *Journal of Climate*, **22**, 4322 – 4335.

Launiainen, S., Guan, M., Salmivaara, A. and Kieloaho, A.-J. (2019) Modeling forest evapotranspiration and water balance at stand and catchment scales: a spatial approach. *Hydrology and Earth System Sciences Discussions*, **2019**, 1–41.

Legates, D. R., Mahmood, R., Levia, D. F., DeLiberty, T. L., Quiring, S. M., Houser, C. and Nelson, F. E. (2011) Soil moisture: A central and unifying theme in physical geography. *Progress in Physical Geography*, **35**, 65–86.

Li, X., McCarty, G. W., Du, L. and Lee, S. (2020) Use of topographic models for mapping soil properties and processes. *Soil Systems*, **4**, 32.

Lin, Y.-S., Medlyn, B. E., Duursma, R. A., Prentice, I. C., Wang, H., Baig, S., Eamus, D., De Dios, V. R., Mitchell, P., Ellsworth, D. S. et al. (2015) Optimal stomatal behaviour around the world. *Nature Climate Change*, **5**, 459–464.

Lohila, A., Aalto, T., Aurela, M., Hatakka, J., Tuovinen, J.-P., Kilkki, J., Penttilä, T., Vuorenmaa, J., Hänninen, P., Sutinen, R. et al. (2016) Large contribution of boreal upland forest soils to a catchment-scale ch4 balance in a wet year. *Geophysical Research Letters*, **43**, 2946–2953.

Maclean, I. M., Bennie, J. J., Scott, A. J. and Wilson, R. J. (2012) A high-resolution model of soil and surface water conditions. *Ecological Modelling*, **237**, 109–119.

Manninen, T., Jääskeläinen, E., Lohila, A., Korkiakoski, M., Räsänen, A., Virtanen, T., Muhić, F., Marttila, H., Ala-Aho, P., Markovaara-Koivisto, M. et al. (2021) Very high spatial resolution soil moisture observation of heterogeneous subarctic catchment using nonlocal averaging and multitemporal sar data. *IEEE Transactions on Geoscience and Remote Sensing*.

Migała, K., Wojtuń, B., Szymański, W. and Muskała, P. (2014) Soil moisture and temperature variation under different types of tundra vegetation during the growing season: A case study from the fuglebekken catchment, sw spitsbergen. *Catena*, **116**, 10–18.

Mohanty, B. P., Cosh, M. H., Lakshmi, V. and Montzka, C. (2017) Soil moisture remote sensing: State-of-the-science. *Vadose Zone Journal*, **16**, 1–9.

Niittynen, P., Heikkinen, R. K. and Luoto, M. (2018) Snow cover is a neglected driver of arctic biodiversity loss. *Nature Climate Change*, **8**, 997–1001.

NLS (2020) National land survey of finland: Topographic database. `https://tiedostopalvelu.maanmittauslaitos.fi/tp/kartta`. Last access: 16 July 2020.

Pearson, R. G., Phillips, S. J., Loranty, M. M., Beck, P. S., Damoulas, T., Knight, S. J. and Goetz, S. J. (2013) Shifts in arctic vegetation and associated feedbacks under climate change. *Nature climate change*, **3**, 673–677.

Penna, D., Borga, M., Norbiato, D. and Dalla Fontana, G. (2009) Hillslope scale soil moisture variability in a steep alpine terrain. *Journal of Hydrology*, **364**, 311–327.

Pirinen, P., Simola, H., Aalto, J., Kaukoranta, J.-P., Karlsson, P. and Ruuhela, R. (2012) *Climatological Statistics of Finland 1981–2010*. Helsinki: Finnish Meteorological Institute.

Planet Team (2017) Planet application program interface: In space for life on earth. `https://api.planet.com`. Last access: 11 November 2020.

Pop, E. W., Oberbauer, S. F. and Starr, G. (2000) Predicting vegetative bud break in two arctic deciduous shrub species, salix pulchra and betula nana. *Oecologia*, **124**, 176–184.

R Development Core Team (2020) The r project for statistical computing. `http://www.r-project.org/`.

Raddatz, T., Reick, C., Knorr, W., Kattge, J., Roeckner, E., Schnur, R., Schnitzler, K.-G., Wetzel, P. and Jungclaus, J. (2007) Will the tropical land biosphere dominate the climate–carbon cycle feedback during the twenty-first century? *Climate dynamics*, **29**, 565–574.

Reick, C., Raddatz, T., Brovkin, V. and Gayler, V. (2013) Representation of natural and anthropogenic land cover change in mpi-esm. *Journal of Advances in Modeling Earth Systems*, **5**, 459–482.

Riihimäki, H., Luoto, M. and Heiskanen, J. (2019) Estimating fractional cover of tundra vegetation at multiple scales using unmanned aerial systems and optical satellite data. *Remote Sensing of Environment*, **224**, 119–132.

Rinke, A., Kuhry, P. and Dethloff, K. (2008) Importance of a soil organic layer for arctic climate: A sensitivity study with an arctic rcm. *Geophysical Research Letters*, **35**.

Robock, A., Vinnikov, K. Y., Srinivasan, G., Entin, J. K., Hollinger, S. E., Speranskaya, N. A., Liu, S. and Namkhai, A. (2000) The global soil moisture data bank. *Bulletin of the American Meteorological Society*, **81**, 1281–1300.

Romano, N. (2014) Soil moisture at local scale: Measurements and simulations. *Journal of Hydrology*, **516**, 6–20.

le Roux, P. C., Aalto, J. and Luoto, M. (2013) Soil moisture's underestimated role in climate change impact modelling in low-energy systems. *Global change biology*, **19**, 2965–2975.

le Roux, P. C. and Luoto, M. (2014) Earth surface processes drive the richness, composition and occurrence of plant species in an arctic–alpine environment. *Journal of Vegetation Science*, **25**, 45–54.

Saleem, J. A. and Salvucci, G. D. (2002) Comparison of soil wetness indices for inducing functional similarity of hydrologic response across sites in illinois. *Journal of Hydrometeorology*, **3**, 80 – 91.

Seibert, J., Stendahl, J. and Sørensen, R. (2007) Topographical influences on soil properties in boreal forests. *Geoderma*, **141**, 139–148.

Seneviratne, S. I., Corti, T., Davin, E. L., Hirschi, M., Jaeger, E. B., Lehner, I., Orlowsky, B. and Teuling, A. J. (2010) Investigating soil moisture–climate interactions in a changing climate: A review. *Earth-Science Reviews*, **99**, 125–161.

Starr, G., Oberbauer, S. F. and Ahlquist, L. E. (2008) The photosynthetic response of alaskan tundra plants to increased season length and soil warming. *Arctic, Antarctic, and Alpine Research*, **40**, 181–191.

Street, L., Shaver, G., Williams, M. and Van Wijk, M. (2007) What is the relationship between changes in canopy leaf area and changes in photosynthetic co2 flux in arctic ecosystems? *Journal of Ecology*, **95**, 139–150.

Sturm, M., Schimel, J., Michaelson, G., Welker, J. M., Oberbauer, S. F., Liston, G. E., Fahnestock, J. and Romanovsky, V. E. (2005) Winter biological processes could help convert arctic tundra to shrubland. *Bioscience*, **55**, 17–26.

Thum, T., Räisänen, P., Sevanto, S., Tuomi, M., Reick, C., Vesala, T., Raddatz, T., Aalto, T., Järvinen, H., Altimir, N. et al. (2011) Soil carbon model alternatives for echam5/jsbach climate model: evaluation and impacts on global carbon cycle estimates. *Journal of Geophysical Research: Biogeosciences*, **116**.

Vereecken, H., Huisman, J., Pachepsky, Y., Montzka, C., van der Kruk, J., Bogena, H., Weihermüller, L., Herbst, M., Martinez, G. and Vanderborght, J. (2014) On the spatio-temporal dynamics of soil moisture at the field scale. *Journal of Hydrology*, **516**, 76–96. Determination of soil moisture: Measurements and theoretical approaches.

Virkkala, A.-M. (2020) *Arctic ecosystems: new insights into knowledge gaps and carbon cycling*. Ph.D. thesis, University of Helsinki, Helsinki.

Wang, L. and Liu, H. (2006) An efficient method for identifying and filling surface depressions in digital elevation models for hydrologic analysis and modelling. *International Journal of Geographical Information Science*, **20**, 193–213.

Western, A. W., Grayson, R. B. and Blöschl, G. (2002) Scaling of soil moisture: A hydrologic perspective. *Annual Review of Earth and Planetary Sciences*, **30**, 149–180.

Wild, J., Kopeckỳ, M., Macek, M., Šanda, M., Jankovec, J. and Haase, T. (2019) Climate at ecologically relevant scales: A new temperature and soil moisture logger for long-term microclimate measurement. *Agricultural and Forest Meteorology*, **268**, 40–47.

Williams, C., McNamara, J. and Chandler, D. (2009) Controls on the temporal and spatial variability of soil moisture in a mountainous landscape: the signature of snow and complex terrain. *Hydrology and Earth System Sciences*, **13**, 1325.

Woo, M.-k., Young, K. L. and Brown, L. (2006) High arctic patchy wetlands: hydrologic variability and their sustainability. *Physical Geography*, **27**, 297–307.

Wood, S. N. (2011) Fast stable restricted maximum likelihood and marginal likelihood estimation of semiparametric generalized linear models. *Journal of the Royal Statistical Society: Series B (Statistical Methodology)*, **73**, 3–36.

Yuan, S. and Quiring, S. M. (2017) Evaluation of soil moisture in cmip5 simulations over the contiguous united states using in situ and satellite observations. *Hydrology and Earth System Sciences*, **21**, 2203–2218.

Zhang, Z., Zimmermann, N. E., Kaplan, J. O. and Poulter, B. (2016) Modeling spatiotemporal dynamics of global wetlands: Comprehensive evaluation of a new sub-grid topmodel parameterization and uncertainties. *Biogeosciences*, **13**, 1387–1408.

Zhu, M., Feng, Q., Qin, Y., Cao, J., Zhang, M., Liu, W., Deo, R. C., Zhang, C., Li, R. and Li, B. (2019) The role of topography in shaping the spatial patterns of soil organic carbon. *Catena*, **176**, 296–305.

Tables

TABLE 1 Geospatial datasets used in the study. Soil layer data are based on field surveys, whereas vegetation types and surficial deposits were classified based on a combination of field and remote sensing data. NDVI (Normalized Difference Vegetation Index) was calculated from a satellite image. Topographical variables were calculated from a Digital Elevation Model (DEM).

Category	Dataset	Data source	Spatial resolution	Time	Reference
Soil	Surficial deposit map	Field survey	0.5 m * 0.5 m	2016–2019	Kemppinen et al. (2018)
	Organic and mineral layer depths	Field survey	Point measurements every 50 m	2016–2018	Kemppinen et al. (2018)
Vegetation	NDVI	Sentinel-2	10 m * 10 m	2019	(ESA, 2021)
	Vegetation type	Field data and PlanetScope	3 m * 3 m	2018	New data
Topography	SAGA Wetness Index	DEM	2 m * 2 m	2016	NLS (2020)
	potential solar radiation	DEM	2 m * 2 m	2016	NLS (2020)

TABLE 2 Growing season (μ) and monthly averages, minimum, maximum and range of Volumetric Water Content (VWC%) in 2018–2019. Values were calculated from the regime average timeseries.

Regime	Model	μ	July	August	September	Min	Range	Max
	Measured	13.5	13.5	12.9	14.5	6.2	15.1	21.3
Xeric	JSBACH	16.7	16.1	16.4	17.9	13.0	6.4	19.4
	SpaFHy	15.4	15.1	14.7	16.6	11.4	9.9	21.3
	Measured	25.5	25.0	24.5	27.1	16.6	15.9	32.5
Mesic	JSBACH	32.9	32.1	32.1	35.4	28.5	11.9	40.4
	SpaFHy	27.3	27.0	27.1	27.9	24.8	10.0	34.8
	Measured	61.4	66.2	54.9	64.1	36.7	44.4	81.1
Hydric	JSBACH	59.7	59.9	58.6	61.1	52.9	12.2	65.1
	SpaFHy	47.7	47.9	46.9	49.2	43.1	9.7	52.8

Figure legends

FIGURE 1 The study setting consists of 50 soil moisture loggers situated to measure the different soil moisture conditions of the landscape ((a), Digital Elevation Map provided by the National Land Survey of Finland 2020). The study area is situated in northwestern Finland ((b), Digital Elevation Map provided by European Union, Copernicus Land Monitoring Service 2020, European Environment Agency). Elevation (a), SAGA Wetness Index (SWI; (c)), and the sum of potential incoming solar radiation in July (kW m^{-2}, (d)) are topography-based variables. High SWI values indicate high wetness values (c). Soil surficial deposits (e) show the distribution of 1) glacial till, 2) peat deposits, 3) fluvial deposits, 4) boulders and 5) rock outcrops. The Normalized Difference Vegetation Index (NDVI; (f)) represents the variation in vegetation cover, with higher values indicating high amounts of photosynthetic plant tissue.

FIGURE 2 Field-quantified (a) and modelled (b) temporal variation of Volumetric Water Content (VWC%) in xeric (20 loggers), mesic (18 loggers) and hydric (10 loggers) moisture regimes in July–September 2018 as well as daily precipitation sum (Finnish Meteorological Insitute, 2020). Logger measurements (a) are shown separately and model results (b) through regime averages and the range within the regime. Variation within JSBACH results was very small and thus, nearly indistinguishable from regime averages.

FIGURE 3 Correlation between modelled and measured time series of VWC% (Volumetric Water Content) in the three soil moisture regimes during during July–September 2018–2019. The x-axis shows temporal variation in the modelled average time series with respect to growing season averages (i.e. with the growing season mean deducted from the values to allow showing all regimes in one figure). The y-axis shows the same for measured regime average time series. The slope s and R^2 of a linear regression are calculated for each regime and the dashed grey line is the 1 : 1 line.

FIGURE 4 Spatial and temporal variation in soil moisture over the study area during July–September 2018–2019. The spatial variation is quantified as average VWC% (Volumetric Water Content) and temporal variation as range of variation. Field measurements are shown over the model results.

FIGURE 5 GAM modelling the statistical relationship between environmental variables and average measured (a) and modelled (b) VWC% (Volumetric Water Content) as well as measured (c) and modelled (d) range of variation during July–September 2018–2019. The environmental variables used were thickness of the organic soil layer in the measurements (cm) and soil porosity in the mechanistic models, proportion of vegetation cover, SAGA Wetness Index (SWI), potential incoming solar radiation (kW $m^{-}2$) and elevation (for measurements). JSBACH does not simulate water flow in the landscape based on topography so SWI was excluded.

TABLE A1 Soil and vegetation parameters used for JSBACH and SpaFHy.

Parameters (unit)		SpaFHy	JSBACH	Note
Soil				
field capacity (%)	coarse	0.2	19.4	
	mixture	0.33	41.8	
	peat	0.6	88	
Saturated hydraulic conductivity (m/s)	coarse	0.0001	1.4E-05	
	mixture	1E-05	1.5E-06	
	peat	5E-05	2E-06	
soil porosity (%)	coarse	40	39.7	
	mixture	50	55.3	
	peat	90	88	
wilting point (%)	coarse	8	8.7	
	mixture	14	14.2	
	peat	11	25.5	
Clapp & Hornberger parameter	coarse		4.7	
	mixture		4.5	
	peat		4	
pore size index	coarse		0.4	
	mixture		0.5	
	peat		0.7	
beta parameter	coarse	3.1		
	mixture	4		
	peat	6		
soil depth (m)	coarse	0.1	0.5	Assigned
	mixture	0.3	0.5	
	peat	0.6	0.6	
Vegetation				
maximum photosynthetic rate (μmol/(m2 s)	deciduous shrubs	11		Starr et al. (2008)
	evergreen shrubs	6		
	sedge	8		
stomatal parameter (kPa0.5)	deciduous shrubs	3.9		Lin et al. (2015)
	evergreen shrubs	1.5		
	sedge	1.8		Lin 2015
light response par. (W/m2)		50		Launiainen et al. (2019)
degree-days for bud-burst		87		Pop et al. (2000)
duration of leaf development (d)		17		
day length for senescene start (h)		15		
duration of leaf senescene (d)		11		
background surface albedo	tundra		0.17	Hagemann (2002)
	mire		0.12	
surface roughness length due to vegetation (m)			0.03	

5.6 Appendices

FIGURE A1 Influence of field capacity on SpaFHy's modelled VWC% (Volumetric Water Content) in peat soil areas.

FIGURE A2 Relationship between organic layer and growing season average Volumetric Water Content (VWC). Pearson's correlation coefficient between the two variables was 0.79.

FIGURE A3 (A) Field-quantified and (b) simulated temporal variation of soil moisture (Volumetric Water Content) in xeric, mesic and hydric moisture regimes in July–September 2019.

FIGURE A4 Transpiration in JSBACH based on vegetation cover.

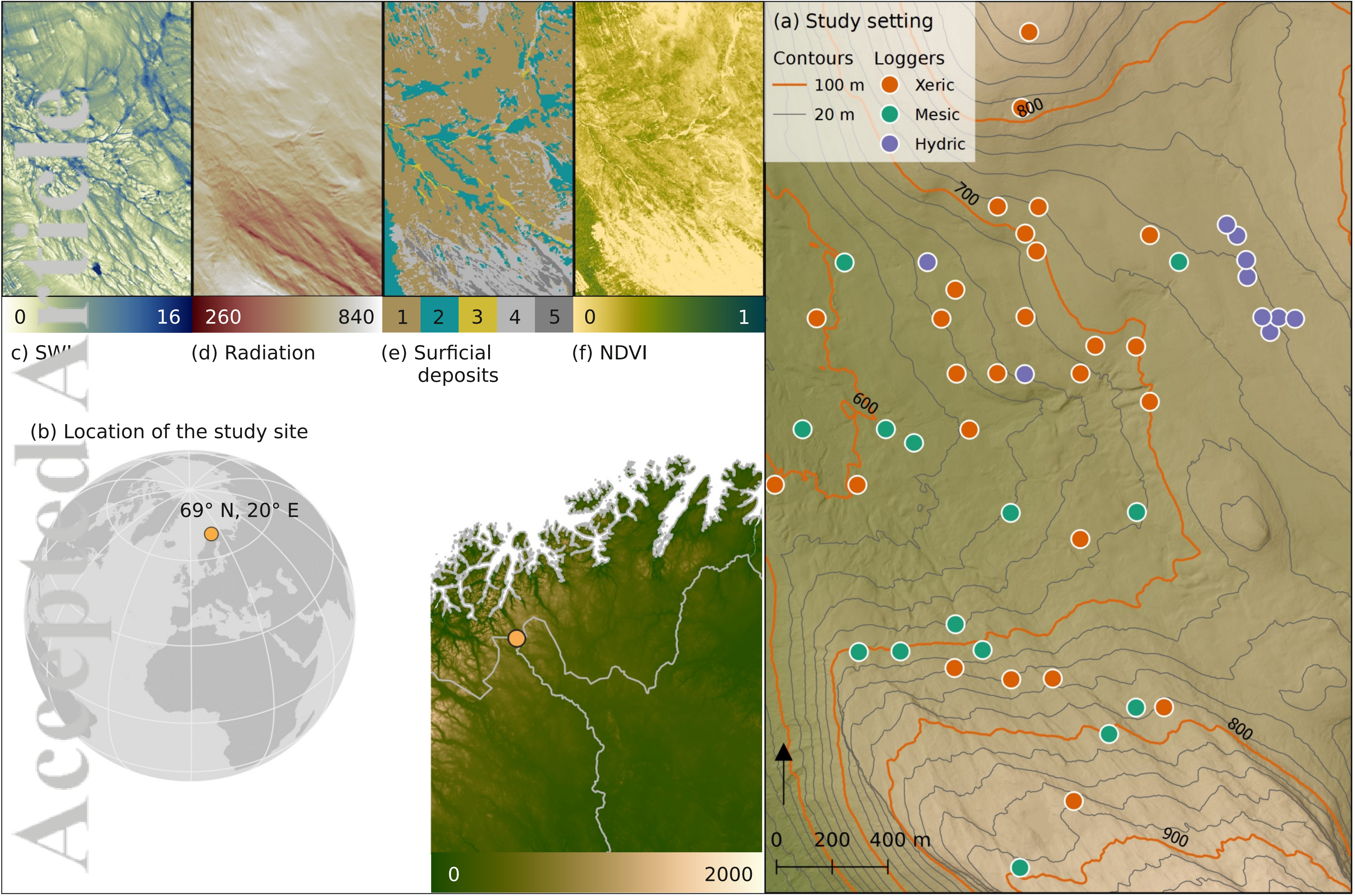
(a) Study setting
Contours
100 m
20 m
Loggers
Xeric
Mesic
Hydric
800
700
600
800
900
0 200 400 m
0
16
c) SWI
260
840
(d) Radiation
1 2 3 4 5
(e) Surficial deposits
0
1
(f) NDVI
(b) Location of the study site
69° N, 20° E
0
2000

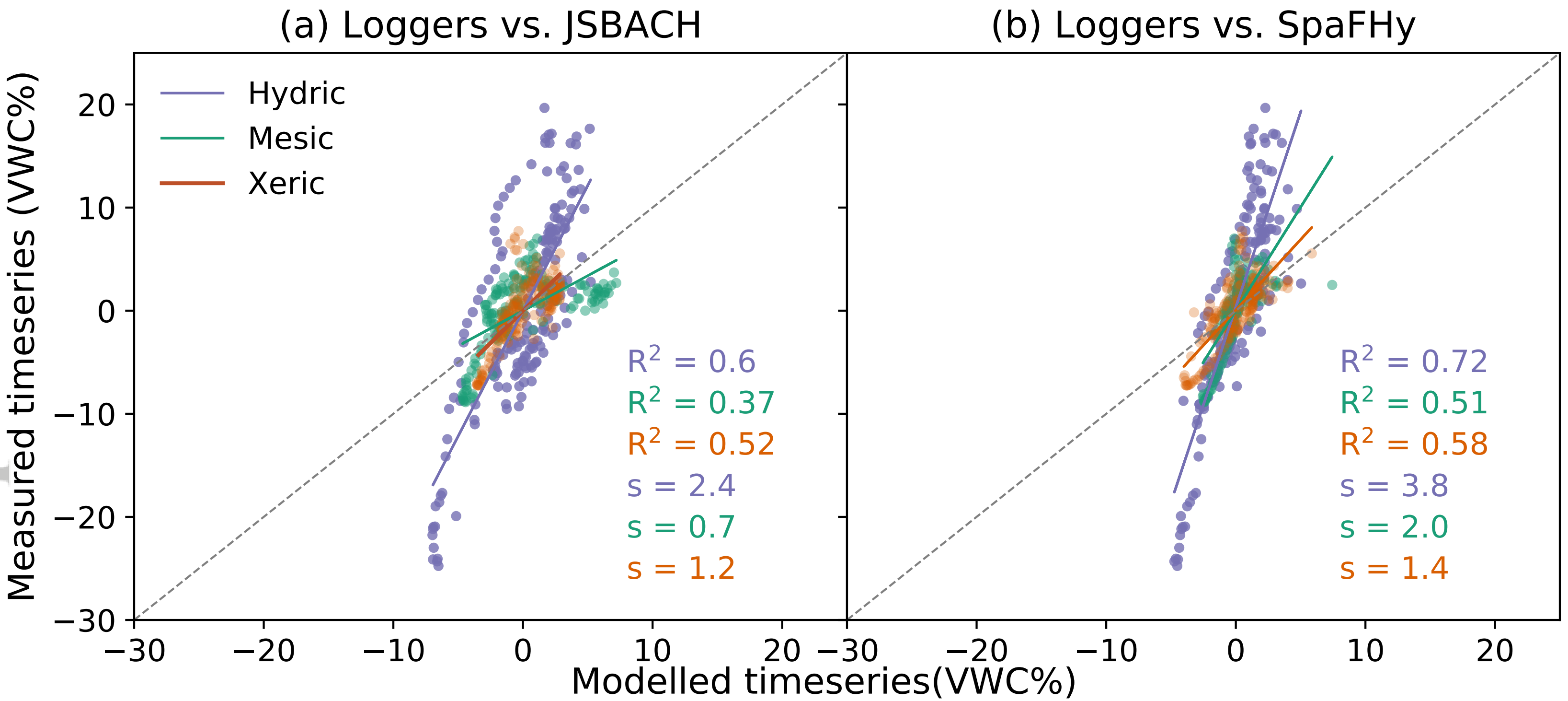
(a) Loggers vs. JSBACH
(b) Loggers vs. SpaFHy
Hydric
Mesic
Xeric
Measured timeseries (VWC%)
Modelled timeseries(VWC%)
R2 = 0.6
R2 = 0.37
R2 = 0.52
s = 2.4
s = 0.7
s = 1.2
R2 = 0.72
R2 = 0.51
R2 = 0.58
s = 3.8
s = 2.0
s = 1.4
20
10
0
−10
−20
−30
−30
−20
−10
0
10
20

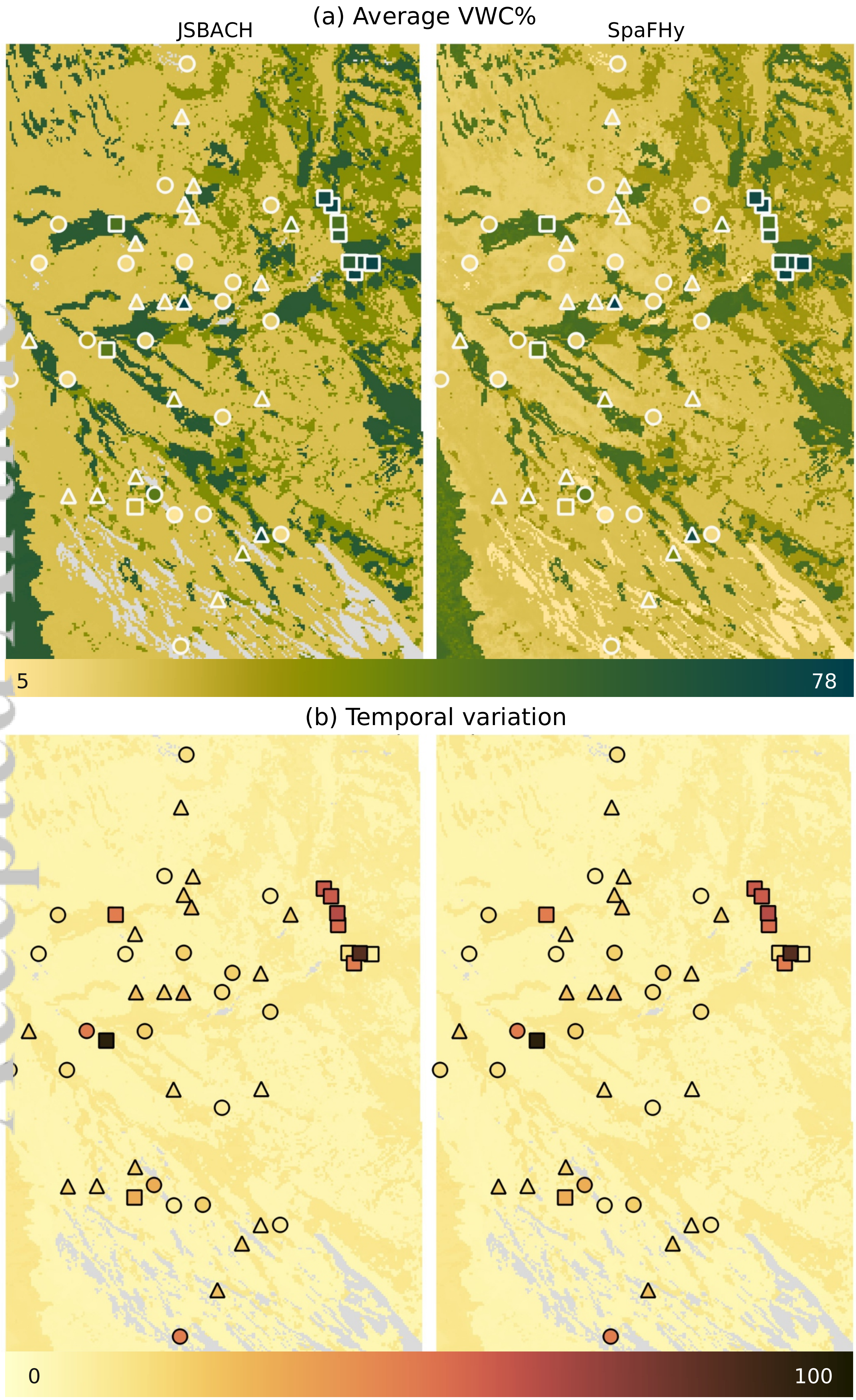

(a) Average VWC%
JSBACH
SpaFHy
5
78
(b) Temporal variation
0
100

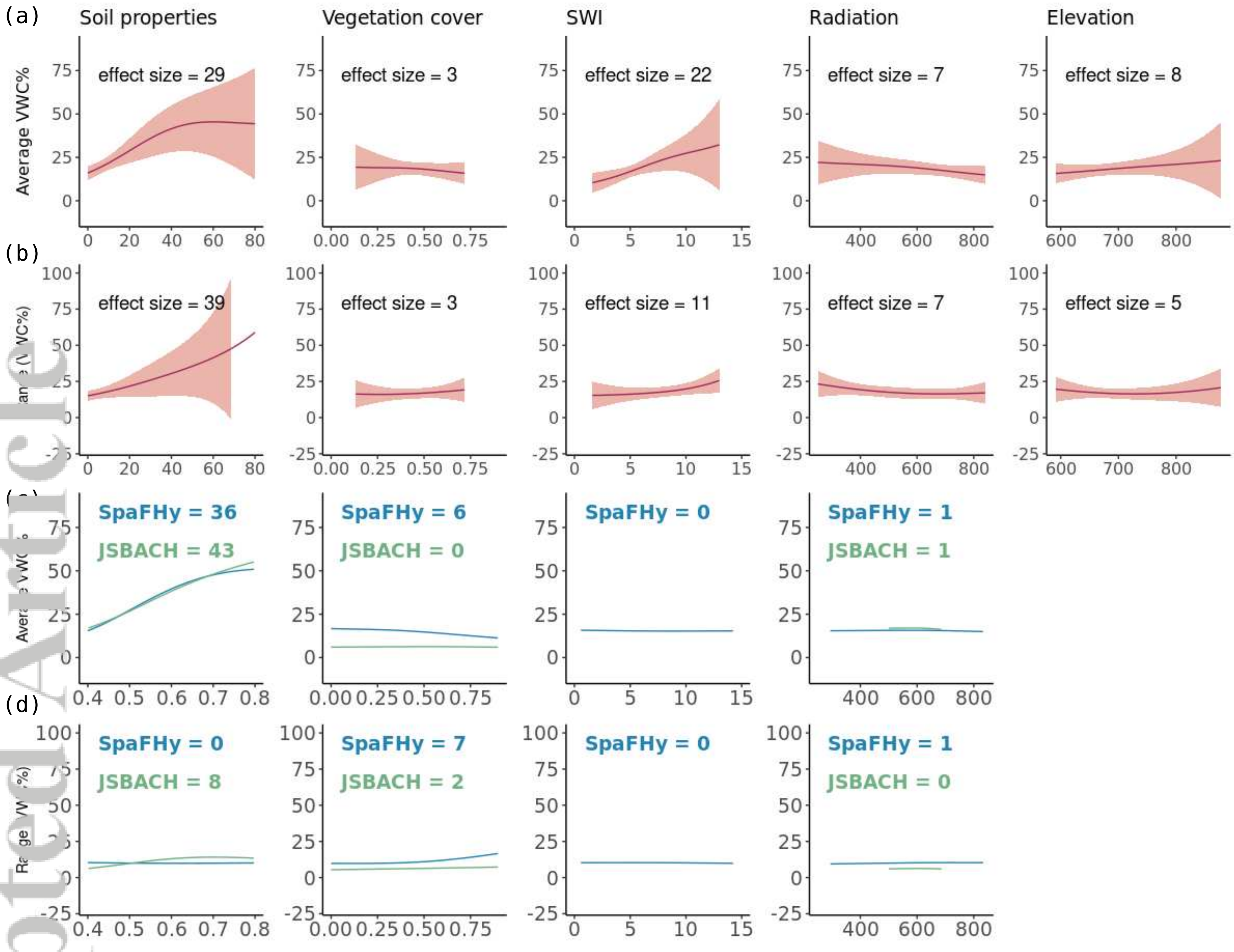

(a)
Soil properties
Vegetation cover
SWI
Radiation
Elevation
Average VWC%
effect size = 29
effect size = 3
effect size = 22
effect size = 7
effect size = 8
(b)
effect size = 39
effect size = 3
effect size = 11
effect size = 7
effect size = 5
(c)
SpaFHy = 36
JSBACH = 43
SpaFHy = 6
JSBACH = 0
SpaFHy = 0
SpaFHy = 1
JSBACH = 1
(d)
SpaFHy = 0
JSBACH = 8
SpaFHy = 7
JSBACH = 2
SpaFHy = 0
SpaFHy = 1
JSBACH = 0

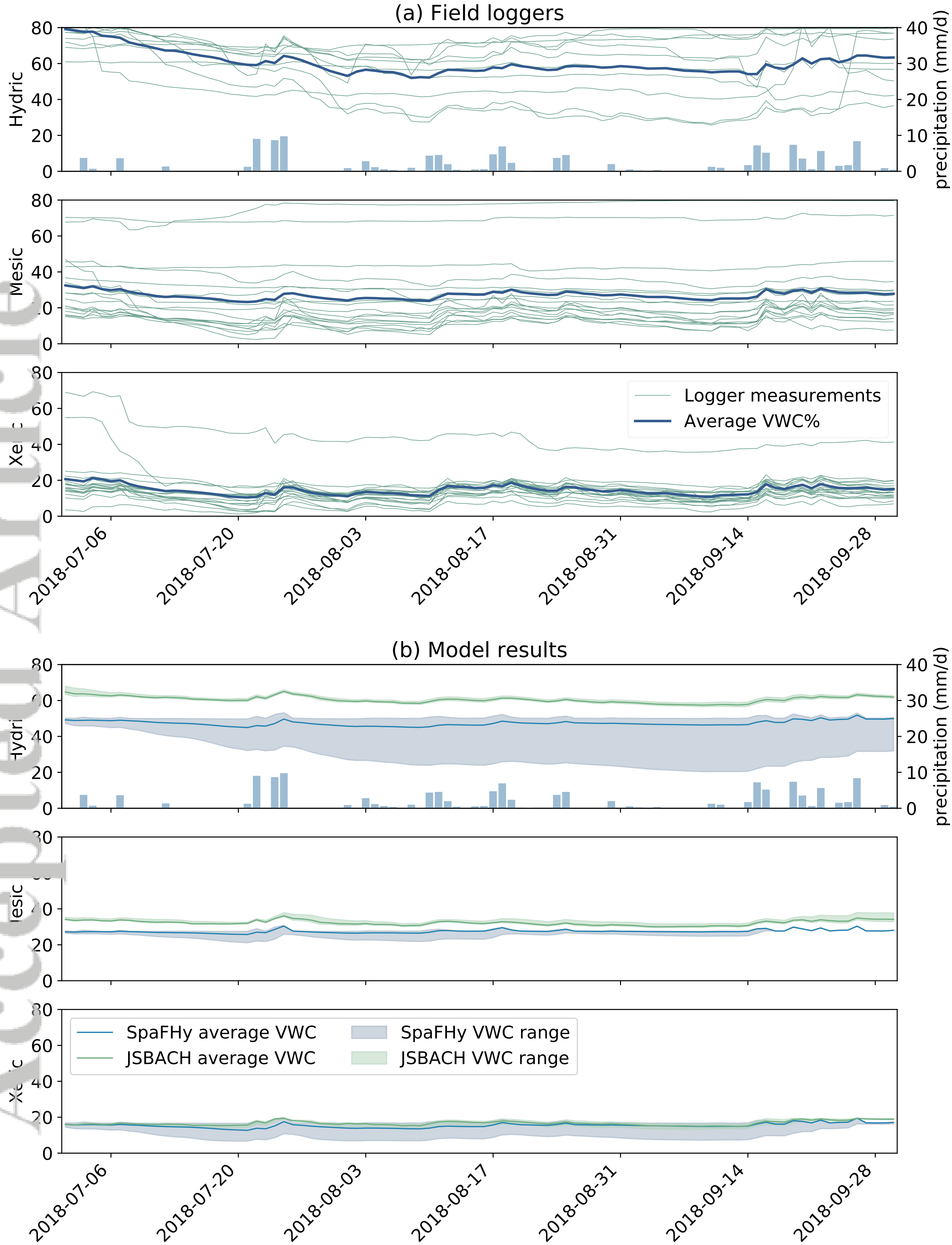

(a) Field loggers
Hydric
Mesic
Xeric
precipitation (mm/d)
Logger measurements
Average VWC%
2018-07-06
2018-07-20
2018-08-03
2018-08-17
2018-08-31
2018-09-14
2018-09-28
(b) Model results
SpaFHy average VWC
JSBACH average VWC
SpaFHy VWC range
JSBACH VWC range

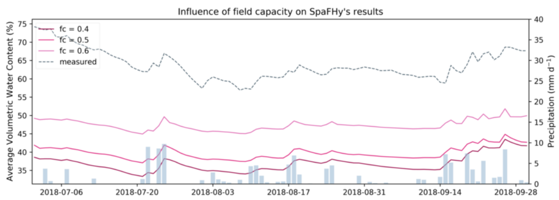

HYP_14450_fig_A01.tif

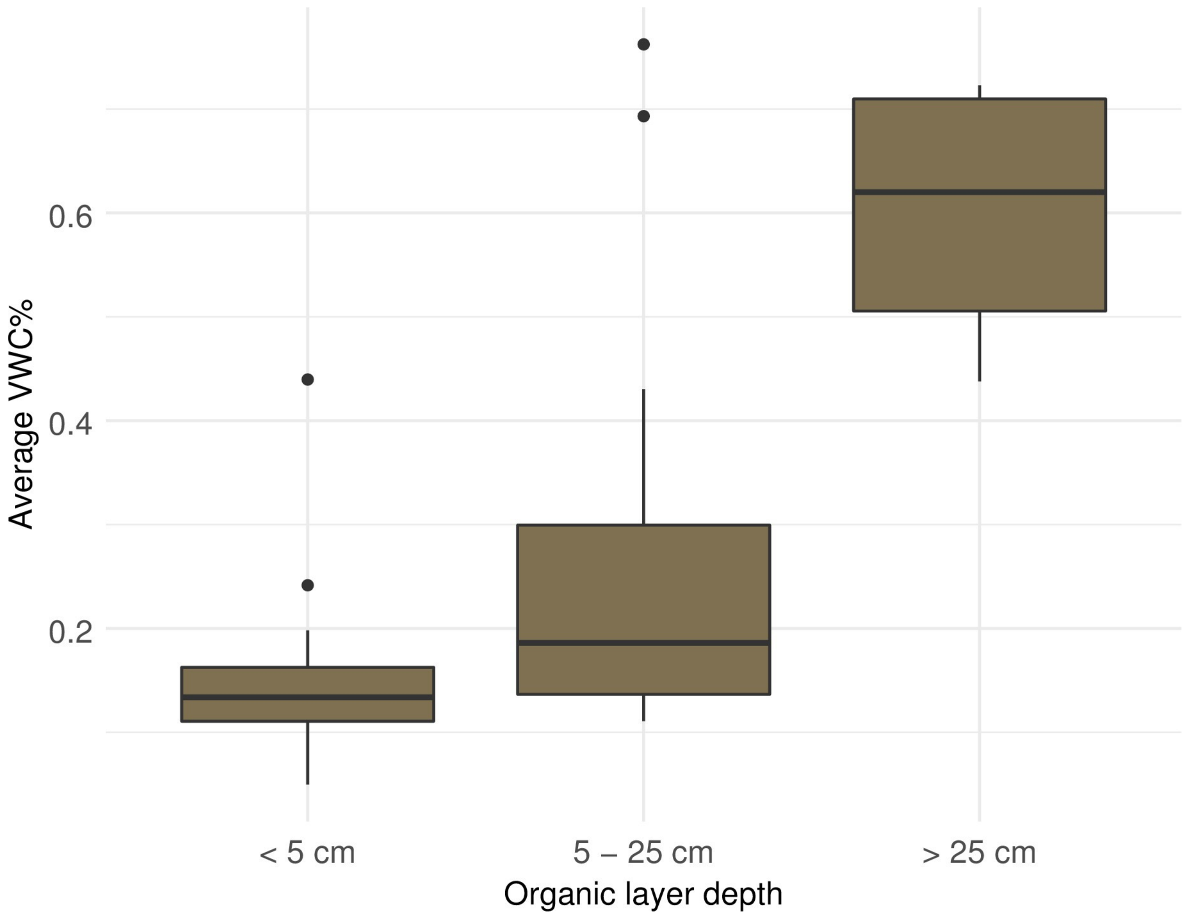

hyp_14450_fig_a02.eps

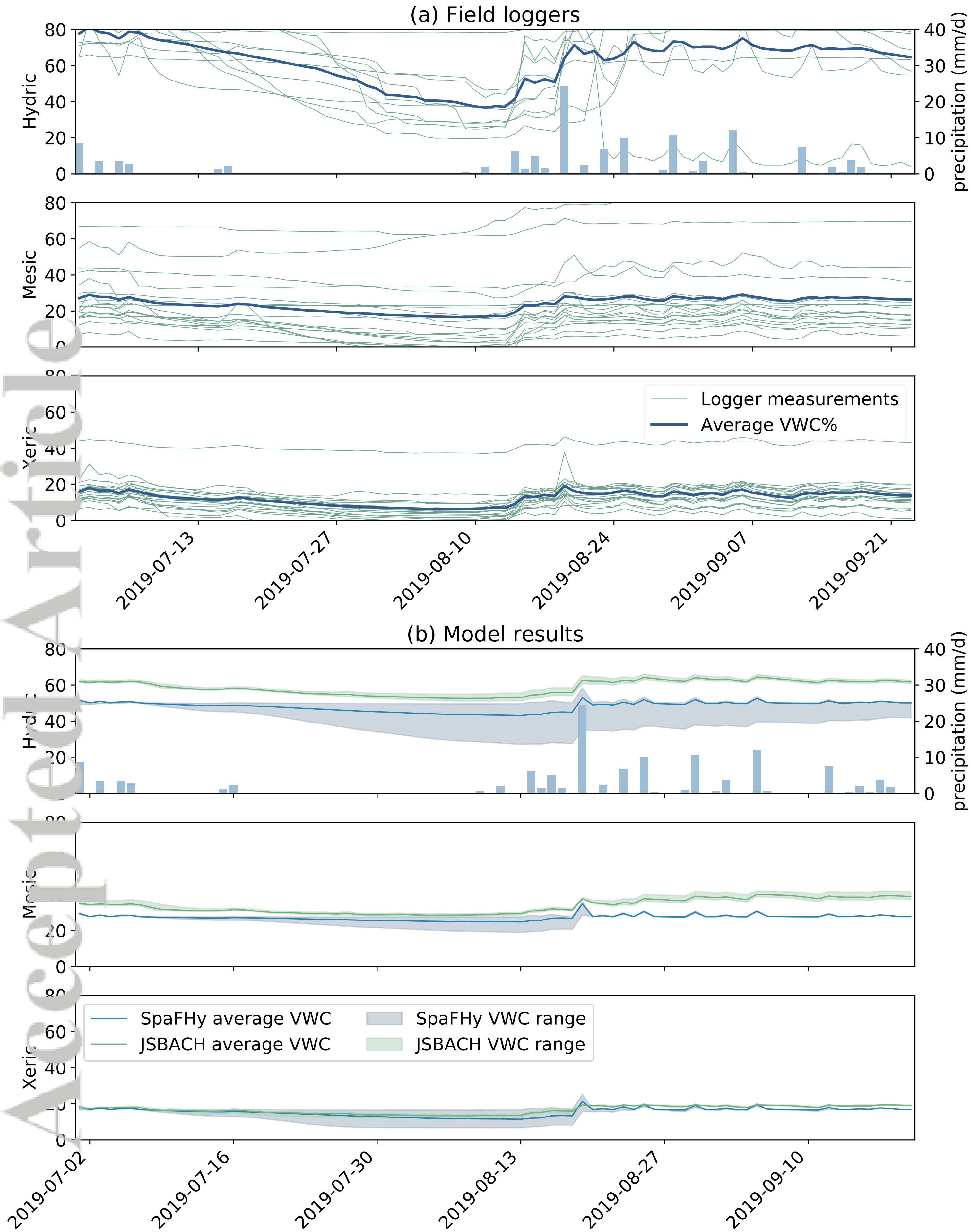

(a) Field loggers
Hydric
Mesic
Xeric
precipitation (mm/d)
Logger measurements
Average VWC%
2019-07-13
2019-07-27
2019-08-10
2019-08-24
2019-09-07
2019-09-21
(b) Model results
SpaFHy average VWC
JSBACH average VWC
SpaFHy VWC range
JSBACH VWC range
2019-07-02
2019-07-16
2019-07-30
2019-08-13
2019-08-27
2019-09-10

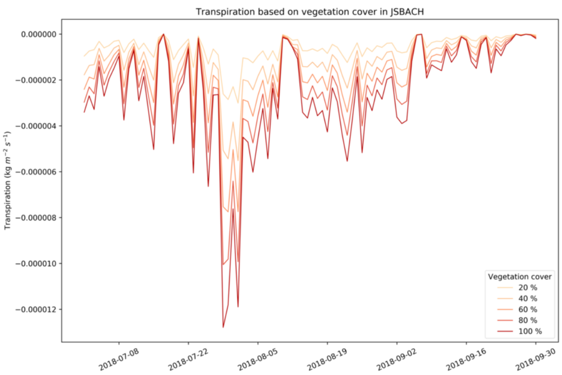

HYP_14450_fig_A04.tif